PAPER • **OPEN ACCESS**

Noise Resilient distributed Voltage and Frequency Control for Low Voltage Islanded Microgrid

To cite this article: S Shrivastava *et al* 2020 *IOP Conf. Ser.: Mater. Sci. Eng.* **937** 012036

View the article online for updates and enhancements.

This content was downloaded from IP address 106.195.38.187 on 05/08/2021 at 11:15

IOP Conf. Series: Materials Science and Engineering **937** (2020) 012036 doi:10.1088/1757-899X/937/1/012036

Noise Resilient distributed Voltage and Frequency Control for Low Voltage Islanded Microgrid

S Shrivastava[1], J Sahu[2] and R Sitharthan[1]

[1]School of Electrical Engineering, Vellore Institute of Technology, Vellore, TN 632014, India

[2]School of Mechanical Engineering, Vellore Institute of Technology, Vellore, TN 632014, India

mailto: sonam24390@gmail.com

Abstract. Motivated by advancement in distributed control schemes of microgrid (MG) network, this paper presents a noise resilient secondary control scheme for low voltage (LV) islanded MG network. For a LV MG the grid lines are highly resistive, hence conventional droop control results in poor stability and power sharing. A combination of droop-boost primary control with a noise resilient secondary distributed control is presented in this work. The presented control scheme achieves accurate power sharing and voltage and frequency restoration under noisy communication links for LV MG network. The communication links used for information sharing in secondary control are subjected to noisy environment; therefore the data received is corrupted with noise. The presented control scheme counteracts the noise effect for LV MG network. The performance of presented control scheme is evaluated by simulating a 4-bus MG test system in MATLAB/SimPowerSystem environment under different test scenarios. The obtained results envisage that the presented control scheme restores the voltage/frequency and provide accurate active power sharing in short time under load perturbation, varying noise parameters, and plug and play operating conditions.

1. Introduction

In the last decade electrical power system has undergone plenty of changes that make it more decentralised to distributed power system. The small scale generators geographically located to the user end at low voltage (LV) level is becoming new trend, which involve more and more renewable energy sources (RESs). These low voltage feeders comprises of several distributed generators (DGs), storage devices and loads appears as a distributed network known as microgrid (MG). The MG can operate either in grid tied mode and support bidirectional power flow or can operate bidirectional power flow or can operate autonomously as a self-regulatory islanded system [1]. Despite having small structure the MG have different operating characteristics than the conventional grid, hence different control structure is required for control and operation of inertia-less, low voltage MG network. The MG control structure is evolved from centralised to decentralized then further aggregated as distributed control structure. A hierarchical three level control is best suited approach for the control of MG network that comprises of primary control level, secondary control level and tertiary control level [2]. The primary control depends on the type of MG network. In this paper a droop-boost control scheme is adapted for achieving accurate power sharing and stable operating voltage and frequency. The secondary control level synchronizes the MG voltage and frequency to

Content from this work may be used under the terms of the Creative Commons Attribution 3.0 licence. Any further distribution of this work must maintain attribution to the author(s) and the title of the work, journal citation and DOI.
Published under licence by IOP Publishing Ltd

nominal values and compensates for the deviations caused by primary control level [3]. The tertiary control level is a supervisory control layer responsible for optimization of power distribution cost and bidirectional power flow optimization [4].

Inspired from the networked control theory of multi agent system (MAS) several distributed control methods are presented in literature which utilizes neighbours information [5, 6]. The accuracy of these control schemes depends upon the grid parameter such as line impedance. A secondary control methodology addressed in [7] works on the presumption of dominant inductive line impedance. For LV MG network these schemes are subjected to power transients and instability [8]. In [7, 9] voltage control is modelled as a tracking synchronization problem while utilizing feedback linearization to convert nonlinear system dynamics of MG to a linear system. The performance of the controller depends on the topology of information sharing, noisy channel of communication, link failure, packet dropout, and communication link delays. Such problems are solved by many researchers using different secondary control approaches. The work in [10] presents a distributed restoration approach for frequency control of MG network. The unmodeled dynamics and effect of communication link delays for islanded MG are addressed in [11, 12] respectively. The information sharing communication topology is of vital importance in operation of distributed secondary control and it affects the controller performance. In [10, 13] address these issues to reduce the MG instability and high oscillations under large signal disturbances for highly inductive MG. In the contrary this paper introduces a noise resilient distributed secondary synchronization scheme for voltage and frequency both in a low voltage MG network. The main contributions of the paper are as follows.

- Noise resilient distributed secondary synchronization scheme is presented for voltage and frequency restoration in a LV MG network.
- The presented controller only uses sparse communication network and is robust against noise parameter uncertainty and high signal disturbance such as loss of DG unit.

The rest of the paper is in the following order. Section II discusses the preliminaries on modelling of LV MG, primary control, and graph theory and communication noise. Section III and IV discusses the presented secondary restoration scheme for output DG voltage and frequency respectively. Case studies for performance evaluation are presented in section V. Conclusion is presented in Section VI.

2. Preliminaries

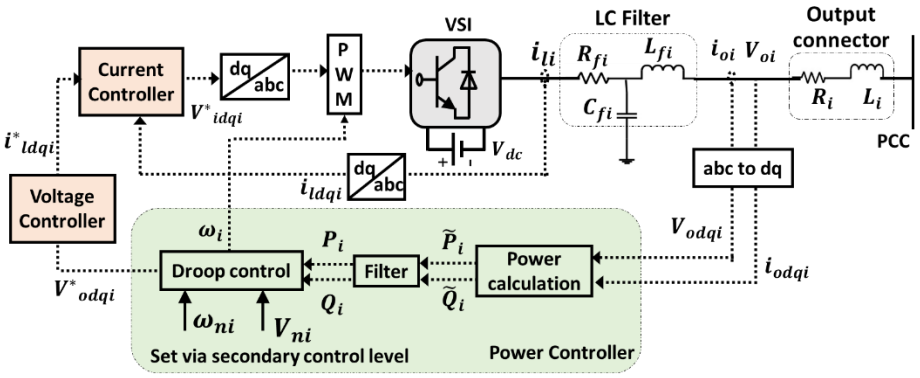

Figure 1. Single line design of VSI based i^{th}DG unit.

2.1. Primary control of low voltage microgrid

The microgrid is a group of interconnected DG units, storage devices and loads. It can be seen as a three layer structure that includes electrical, control and communication layers. The electrical layer consists of a DG unit, transmission lines, energy storage element and loads. Figure 1 shows the one

line diagram of a DG unit. The DG unit consist of DC output voltage of renewable energy source unit, inverter, filter (LC) and output RL connector. The control scheme is of DG is a hierarchical one which includes three layers primary, secondary and tertiary control. The primary layer has three control loops i.e., voltage control loop, output of which is fed to current control loop and power control loops to implement the droop control. The primary droop control dynamics for DGs units can be given as,

$$\omega_i = \omega_{ni} - m_{Pi}^{\omega} P_i \tag{1}$$

$$V_i = V_{ni} - n_{Qi}^{V} Q_i \tag{2}$$

where V_{ni} and ω_{ni} are reference voltage magnitude and angular frequency; P_i and Q_i are real and reactive power; m_{Pi}^{ω} and n_{Qi}^{V} are droop coefficients of i^{th} DG unit respectively.

However, in case of low voltage MG network, the line impedance is highly resistive in nature where operating frequency and DG output voltages are closely associated to real and reactive power [15]. Hence, the modified droop-boost characteristics for primary control is given as,

$$\omega_i = \omega_{ni} + k_Q^{\omega} Q_i \tag{3}$$

$$V_i = V_{ni} - k_P^{V} P_i \tag{4}$$

where k_Q^{ω} and k_P^{V} are boost and droop coefficients for frequency and output voltage control respectively. The model for DG unit with its inner control loop can be given as [14]

$$\frac{dx_i}{dt} = \psi_i(x_i) + g_i^{V}(x_i)\, u_i^{V} + g_i^{\omega}(x_i)\, u_i^{\omega} + k_i(x_i) D_i \tag{5}$$

$$y_{iV} = h_{iV}(x_i) = V_i \tag{6}$$

$$y_{i\omega} = h_{i\omega}(x_i) + d_i u_i^{\omega} = \omega_i = \omega_{ni} + k_Q^{\omega} Q_i \tag{7}$$

where $x_i = \left[\alpha_i, P_i, Q_i, i_{ldi}, i_{lqi}, V_{odi}, V_{oqi}, i_{odi}, i_{oqi}\right]^T$; α_i is angle of DG reference frame; $x_i = \left[\omega_{ref}, V_{bdi}, V_{qdi}\right]^T$ is known disturbance. The secondary control inputs for primary droop-boost control level will be discussed in next section. This control layer synchronizes the output DG voltage and operating frequency to their nominal values.

2.2. Preface on graph theory

The adaptation of graph theory is taken from the work in [6]. A weighted, non-directional and well-connected graph $\mathcal{G} = \left(\mathcal{V}_{\mathcal{G}}, \mathrm{E}_{\mathcal{G}}, \mathrm{A}_{\mathcal{G}}\right)$, with $\mathcal{V}_{\mathcal{G}}$ as set of nodes, i.e., $\{1, \ldots, \mathrm{N}\}$, $\mathrm{E}_{\mathcal{G}}$ is set of edges, i.e., $\mathrm{E}_{\mathcal{G}} \subseteq \left(\mathcal{V}_{\mathcal{G}} \times \mathcal{V}_{\mathcal{G}}\right)$, $\mathrm{A}_{\mathcal{G}}$ is weighted adjacency matrix. For an edge $(\mathrm{i}, \mathrm{j}) \in \mathrm{E}_{\mathcal{G}}$, $\mathrm{a_{ij}} = \mathrm{a_{ij}} = 1$, else $\mathrm{a_{ij}} = \mathrm{a_{ij}} = 0$. The degree matrix $\mathcal{D} = \mathrm{Diag}\{\mathrm{d_i}\}$ of graph , where $\mathrm{d_i} = \sum_{\mathrm{j} \in \mathcal{N}_\mathrm{i}} \mathrm{a_{ij}}$. $\mathcal{N}_\mathrm{i}$ is the set of neighbouring DG units defined as $\mathcal{N}_\mathrm{i} = \left\{\mathrm{j} \in \mathcal{V}_{\mathcal{G}} : (\mathrm{i}, \mathrm{j}) \in \mathrm{E}_{\mathcal{G}}, \mathrm{j} \notin \mathrm{i}\right\}$. The Laplacian matrix $\mathcal{L}_{\mathcal{G}} = \mathcal{D} - \mathrm{A}_{\mathcal{G}}$.

2.3. Preface on communication noise

In secondary control layer, the communication between the agents is compulsory requirement. The communication link irrespective of its type is impaired with the noise due to cyber-attack, sensor uncertainty and climate conditions. In this work, generalized Gaussian noise is considered to simulate the noisy communication links between DGs. The probability distribution function (PDF) for noise considered in this work is given as [14]

$$p\big(n(t)\big) = \frac{1}{\sqrt{2\pi\sigma^2}} exp\left(\frac{-1}{2\sigma^2}\Big(n(t) - mean\big(n(t)\big)\Big)^2\right) \tag{8}$$

where σ^2 is the noise signal variance of $n(t)$. Various PDFs of communication noise with different noise variances are shown in figure 2, where mean is zero.

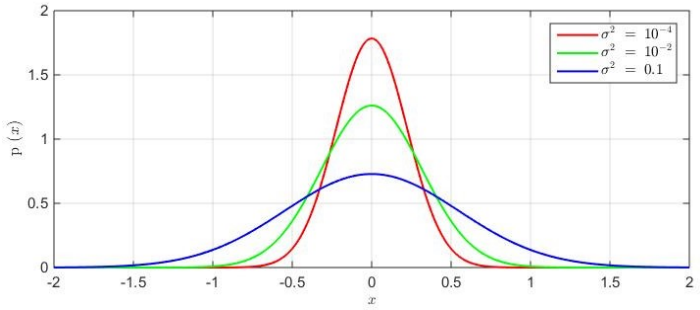

Figure 2. Probability distribution function of AWGN with different variance.

3. Distributed noise resilient voltage control

Feedback linearization is employed to convert the nonlinear DG system dynamics of $\boldsymbol{i^{th}}$ DG into linear system. The state space model of voltage control for MG network in matrix form is given as follows [10, 14]

$$\dot{\boldsymbol{y}}_{\boldsymbol{iV}} = \boldsymbol{A}\boldsymbol{y}_{\boldsymbol{iV}} + \boldsymbol{B}\boldsymbol{u}_{\boldsymbol{i}}^{\boldsymbol{V}}, \forall\, \boldsymbol{i} \tag{9}$$

where, $\boldsymbol{y}_{\boldsymbol{iV}} = \begin{bmatrix} \boldsymbol{y}_{\boldsymbol{iV}} & \boldsymbol{y}_{\boldsymbol{iV},1} \end{bmatrix}^{\boldsymbol{T}}$; $\boldsymbol{B} = [\boldsymbol{0} \quad \boldsymbol{1}]^{\boldsymbol{T}}$; and $\boldsymbol{A} = \begin{bmatrix} \boldsymbol{0} & \boldsymbol{1} \\ \boldsymbol{0} & \boldsymbol{0} \end{bmatrix}$. Also, the leader dynamics $\dot{\boldsymbol{y}}_{\boldsymbol{0}} = \boldsymbol{A}_{\boldsymbol{0}}\boldsymbol{y}_{\boldsymbol{0}}(\boldsymbol{t})$, with $\boldsymbol{y}_{\boldsymbol{0}} = [\boldsymbol{V}_{\boldsymbol{nom}} \quad \boldsymbol{0}]^{\boldsymbol{T}}$; $\boldsymbol{u}_{\boldsymbol{i}}^{\boldsymbol{V}} = \boldsymbol{\psi}_{\boldsymbol{i}}(\boldsymbol{x}_{\boldsymbol{i}}) + \boldsymbol{g}_{\boldsymbol{i}}^{\boldsymbol{V}}(\boldsymbol{x}_{\boldsymbol{i}})\, \boldsymbol{u}_{\boldsymbol{i}}$; with $\boldsymbol{u}_{\boldsymbol{i}}$ denoted the voltage control input.

Considering a low voltage MG being a networked multi-agent system (MAS) with $\boldsymbol{N}$ DG units modelled into agents. The noisy communication channel links existing between the agents causes inaccurate output voltage and operating frequency regulation. Assuming the measured voltage information states depraved with noise can be given as.

$$\tilde{\boldsymbol{y}}_{\boldsymbol{iV}}(\boldsymbol{t}) = \boldsymbol{y}_{\boldsymbol{iV}}(\boldsymbol{t}) + \boldsymbol{\rho}_{\boldsymbol{i}}(\boldsymbol{t}), \boldsymbol{i} = \boldsymbol{1}, \dots, \boldsymbol{N} \tag{10}$$

where $\boldsymbol{\rho}_{\boldsymbol{i}}(\boldsymbol{t})$ is the noise uncertainty. In this paper, we have assumed Additive White Gaussian Noise (AWGN) with $\boldsymbol{mean} = \boldsymbol{0}$ and $\boldsymbol{\sigma^2}$ as variance.

The noise resilient secondary synchronization control law can be designed as [14]

$$\boldsymbol{u}_{\boldsymbol{i}}^{\boldsymbol{V}} = -\boldsymbol{C}_{\boldsymbol{0V}}\tilde{\boldsymbol{y}}_{\boldsymbol{i}}(\boldsymbol{t}) - \boldsymbol{\alpha}_{\boldsymbol{V}}\boldsymbol{C}_{\boldsymbol{V}}\left[\sum_{\boldsymbol{j}\in\mathcal{N}_{\boldsymbol{i}}}\left(\tilde{\boldsymbol{y}}_{\boldsymbol{i}}(\boldsymbol{t}) - \tilde{\boldsymbol{y}}_{\boldsymbol{j}}(\boldsymbol{t})\right) + \boldsymbol{q}_{\boldsymbol{i}}\left(\tilde{\boldsymbol{y}}_{\boldsymbol{i}}(\boldsymbol{t}) - \boldsymbol{y}_{\boldsymbol{0}}(\boldsymbol{t})\right)\right] + \boldsymbol{\delta}_{\boldsymbol{i}}^{\boldsymbol{V}}(\boldsymbol{t}) \tag{11}$$

where $\boldsymbol{\delta}_{\boldsymbol{i}}^{\boldsymbol{V}}(\boldsymbol{t})$ is the corrective auxiliary control signal to attenuate the noise effect.

The noise auxiliary control signal is designed as [14]

$$\boldsymbol{\delta}_{\boldsymbol{i}}^{\boldsymbol{V}}(\boldsymbol{t}) = \boldsymbol{C}_{\boldsymbol{0V}}\hat{\boldsymbol{\rho}}_{\boldsymbol{i}}(\boldsymbol{t}) + \boldsymbol{\alpha}_{\boldsymbol{V}}\boldsymbol{C}_{\boldsymbol{V}}\left[\sum_{\boldsymbol{j}\in\mathcal{N}_{\boldsymbol{i}}}\left(\hat{\boldsymbol{\rho}}_{\boldsymbol{i}}(\boldsymbol{t}) - \hat{\boldsymbol{\rho}}_{\boldsymbol{j}}(\boldsymbol{t})\right) + \boldsymbol{q}_{\boldsymbol{i}}\left(\hat{\boldsymbol{\rho}}_{\boldsymbol{i}}(\boldsymbol{t})\right)\right] \tag{12}$$

where

$$\dot{\hat{\boldsymbol{\rho}}}_{\boldsymbol{i}} = -\boldsymbol{\beta}_{\boldsymbol{V}}\boldsymbol{A}^{\boldsymbol{T}}\boldsymbol{P}\left(\tilde{\boldsymbol{y}}_{\boldsymbol{i}}(\boldsymbol{t}) - \hat{\boldsymbol{y}}_{\boldsymbol{i}}(\boldsymbol{t}) - \hat{\boldsymbol{\rho}}_{\boldsymbol{i}}(\boldsymbol{t})\right), \boldsymbol{t} \geq \boldsymbol{0} \tag{13}$$

and

$$\dot{\hat{\boldsymbol{y}}}_{\boldsymbol{i}}(\boldsymbol{t}) = \boldsymbol{A}_{\boldsymbol{0}}\hat{\boldsymbol{y}}_{\boldsymbol{i}}(\boldsymbol{t}) - \boldsymbol{\alpha}_{\boldsymbol{V}}\boldsymbol{B}\boldsymbol{C}_{\boldsymbol{V}}\left[\sum_{\boldsymbol{j}\in\mathcal{N}_{\boldsymbol{i}}}\left(\hat{\boldsymbol{y}}_{\boldsymbol{i}}(\boldsymbol{t}) - \hat{\boldsymbol{y}}_{\boldsymbol{j}}(\boldsymbol{t})\right) + \boldsymbol{q}_{\boldsymbol{i}}\left(\hat{\boldsymbol{y}}_{\boldsymbol{i}}(\boldsymbol{t}) - \boldsymbol{y}_{\boldsymbol{0}}(\boldsymbol{t})\right)\right] + \left(\boldsymbol{\beta}_{\boldsymbol{V}}\boldsymbol{A}^{\boldsymbol{T}}\boldsymbol{P} + \boldsymbol{\gamma}_{\boldsymbol{V}}\boldsymbol{I}_{\boldsymbol{N}}\right)\left(\tilde{\boldsymbol{y}}_{\boldsymbol{i}}(\boldsymbol{t}) - \hat{\boldsymbol{y}}_{\boldsymbol{i}}(\boldsymbol{t}) - \hat{\boldsymbol{\rho}}_{\boldsymbol{i}}(\boldsymbol{t})\right), \boldsymbol{t} \geq \boldsymbol{0} \tag{14}$$

with β_V and γ_V are design coefficients; $\hat{\rho}_i(t)$ and $\hat{y}_i(t)$ are the estimated values for noise and corrupted state for i^{th} DG unit; P is solution of linear matrix inequality and given as

$$I_N \otimes (A_0^T P + P A_0 - 2\gamma_V P) - \alpha_V \mathcal{F}_\mathcal{G} \otimes (C_V^T B^T P + P B C_V) < 0 \quad (15)$$

3.1. Theorem 1

A N DG unit networked MAS with connected undirected graph $\mathcal{G}$ is considered with dynamics given in equation (5) to equation (7). The control protocol designed in equation (12) and (13) provide a Lyapunov stable system, while restoring the voltage magnitude to nominal value i.e., $V_{ref} = 230\,V$ under noisy communication channel for LV MG.

3.2. Proof

The compact for of controller designed in equation (12) can be obtained using equation (9) as follows

$$\dot{y}(t) = \left[I_N \otimes A_0 - \alpha_V \mathcal{F}_\mathcal{G} \otimes B C_V\right] y(t) + \left(\alpha_V G_\mathcal{G} \otimes B C_V\right) y_0(t) - (I_N \otimes A)\rho + (I_N \otimes B)\delta^V(t), t \geq 0 \quad (16)$$

where $y(t) = [y_1^T(t), \dots, y_N^T(t)]^T$, $\rho = [\rho_1^T, \dots, \rho_N^T]^T$, and $\delta^V(t) = [\delta_1^T(t), \dots, \delta_N^T(t)]^T$. The compact form of $\hat{y}(t)$ can be given as

$$\dot{\hat{y}}(t) = \left[I_N \otimes A_0 - \alpha_V \mathcal{F}_\mathcal{G} \otimes B C_V\right] \hat{y}(t) + \left(\alpha_V G_\mathcal{G} \otimes B C_V\right) y_0(t) - \left(\alpha_V \mathcal{F}_\mathcal{G} \otimes B C_V + I_N \otimes B C_0\right) \hat{\rho} + (I_N \otimes B)\delta^V(t) + \psi(t), t \geq 0 \quad (17)$$

where $\hat{y}(t) = [\hat{y}_1^T(t), \dots, \hat{y}_N^T(t)]^T$ and $\psi(t) = [\psi_1^T(t), \dots, \psi_N^T(t)]^T$ with $\psi_i(t) = -\dot{\hat{\rho}}_i(t) + \gamma_V e_i(t)$.

Defining global error vector as $e_i(t) = \tilde{y}_i(t) - \hat{y}_i(t) - \hat{\rho}_i(t)$ and $\tilde{\rho}_i(t) = \rho_i - \hat{\rho}_i(t)$, and their compact form can be given as follows

$$\tilde{\rho}(t) = (I_N \otimes \beta_V A^T P) e(t), t \geq 0 \quad (18)$$

$$\dot{e}(t) = (A_e - \gamma_V I_N) e(t) - (I_N \otimes A)\tilde{\rho}(t), t \geq 0 \quad (19)$$

where $A_e = I_N \otimes A_0 - \alpha_V \mathcal{F}_\mathcal{G} \otimes B C_V$ and $e(t) = [e_1^T(t), \dots, e_N^T(t)]^T$ and $\tilde{\rho}(t) = [\tilde{\rho}_1^T(t), \dots, \tilde{\rho}_N^T(t)]^T$.

Based on the findings in [14], the Lyapunov stability of equation (18) and equation (19) is comparable with the control scheme's Lyapunov stability presented in equation (11) in terms of Lyapunov criterion. Considering the Lyapunov stability equation as

$$V(e, \tilde{\rho}) = \sum_{i=1}^{N} \left(e_i^T P e_i + \beta_V^{-1} \tilde{\rho}_i^T \tilde{\rho}_i\right) = e^T (I_N \otimes P) e + \beta_V^{-1} \tilde{\rho}^T \tilde{\rho} \quad (20)$$

Now finding the time derivative of equation (20) along the trajectories of (18) and (19) gives

$$\dot{\mathrm{V}}(\mathrm{e}, \tilde{\sigma}) = \mathrm{e}^{\mathrm{T}} \left(\mathrm{I_N} \otimes \left(\mathrm{A_0^T P + P A_0 - 2\gamma_V P}\right) - \alpha_\mathrm{V} \mathcal{F}_\mathcal{G} \otimes \left(\mathrm{C_V^T B^T P + P B C_V}\right)\right) \mathrm{e} \leq 0, \mathrm{t} \geq 0 \quad (21)$$

Now following the approach similar to [14], it can be shown that $\left(\mathrm{I_N} \otimes \left(\mathrm{A_0^T P + P A_0 - 2\gamma_V P}\right) - \alpha_\mathrm{V} \mathcal{F}_\mathcal{G} \otimes \left(\mathrm{C_V^T B^T P + P B C_V}\right)\right)$ is Hurwitz. Hence, equation (18) and equation (19) are Lyapunov stable for all $(\mathrm{e}_0, \tilde{\rho}_0) \in \mathbb{R}_\mathrm{N} \times \mathbb{R}_\mathrm{N}$. This concludes the proof.

3.3. Remark 1

Using Theorem 1, $\lim_{t \to \infty} \tilde{\rho}(t) = 0$, and $\lim_{t \to \infty} e(t) = 0$, implies that $\lim_{t \to \infty} \left(y(t) - \hat{y}(t)\right) = 0$, i.e., state estimate $\hat{y}(t)$ coincide to the correct information state $y(t)$ for $t \geq 0$. Hence, presented controller in equation (11) guarantees voltage restoration for all DGs to nominal value for LV MG with noisy communication link.

4. Distributed noise-resilient frequency control

In this section a distributed secondary noise resilient operating frequency control input is presented using a analogous approach adapted in section 3. Defining the auxiliary control input after feedback linearization as follows

$$\boldsymbol{y_{i\omega} = \dot{\omega}_i = \dot{\omega}_{ni} + k_Q^{\omega} Q_i = u_i^{\omega}} \tag{22}$$

The corrupted measured frequency state is considered as follows

$$\tilde{y}_{i\omega}(t) = y_{i\omega}(t) + \rho_i(t), i = 1, \ldots, \mathrm{N} \tag{23}$$

The secondary noise resilient frequency control signal with the auxiliary corrective control signal can be devised as follows [14]

$$\boldsymbol{u_i^{\omega} = -C_{0\omega}\tilde{y}_{i\omega}(t) - \alpha_{\omega}C_{\omega}\left[\sum_{j\in\mathcal{N}_i}\left(\tilde{y}_{i\omega}(t) - \tilde{y}_{j\omega}(t)\right) + q_i\left(\tilde{y}_{i\omega}(t) - y_{0\omega}(t)\right)\right] + \delta_i^{\omega}(t)} \tag{24}$$

and

$$\boldsymbol{\delta_i^{\omega}(t) = C_{0\omega}\hat{\rho}_i(t) + \alpha_{\omega}C_{\omega}\left[\sum_{j\in\mathcal{N}_i}\left(\hat{\rho}_i(t) - \hat{\rho}_j(t)\right) + q_i\left(\hat{\rho}_i(t)\right)\right]} \tag{25}$$

4.1. Theorem 2

The controller presented in equation (24) and equation (25) restores the operating frequency of all DG units to the nominal value under noisy communication link for a LV MG network, while guaranteeing accurate active power sharing among DGs.

4.2. Proof

This theorem can be proved similar to the Theorem 1.

5. Performance evaluation

The time domain case studies using MATLAB/Simulink framework in this section envisage the validity of the presented noise resilient secondary layer control scheme for islanded LV MG system (230 Volts, 50 Hz) as shown in figure. 3. The presented scheme is suitable for any communication topology with arbitrary N DG units. The test system and proposed control parameters are given in table 1 and table 2 respectively. The one line MG test system and communication network topology considered for information sharing is given in figure 3 and figure 4 respectively. The parameters of noise resilient distributed secondary control are selected as follows. $\alpha_V = 200$, $\beta_V = 40$, $\gamma_V = 80$, $\alpha_\omega = 200$, $\beta_V = 80$, and $\gamma_\omega = 100$. The reference operating voltage magnitude and frequency are $V_{ref} = 230\,V$ and $f_{ref} = 50\,Hz$ respectively.

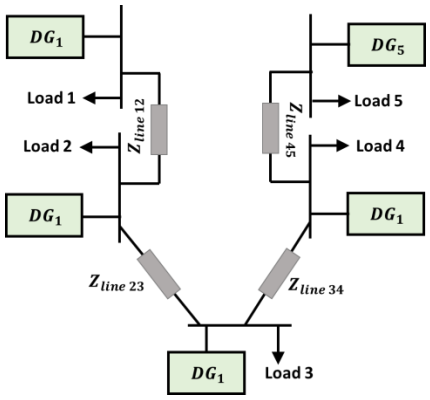

Figure 3. One line diagram test MG system.

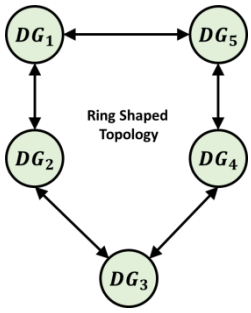

Figure 4. Communication graph.

5.1. Robustness to load perturbation

This case study shows the effectiveness of presented control scheme with load changing environment. The droop-boost primary control layer active with the start of simulation and the secondary control scheme is activated at

Table 1. Parameters of MG test system.

		DG #1 & DG #2 & DG #3				DG #4 & DG #5			
DGs	k_P^ω	9.4×10^{-5}				k_P^ω	12.5×10^{-5}		
	k_Q^v	1.3×10^{-3}				k_Q^v	1.5×10^{-3}		
	R_i	0.03Ω				R_i	0.03Ω		
	L_i	0.35mH				L_i	0.35mH		
	R_f	0.1Ω				R_f	0.5Ω		
	L_f	1.35mH				L_f	0.27mH		
	C_f	50μF				C_f	50μF		
	K_{PV}	0.1				K_{PV}	0.05		
	K_{IV}	420				K_{IV}	390		
	K_{PC}	15				K_{PC}	10.5		
	K_{IC}	20000				K_{IC}	16000		
Lines		$Z_{Line\,12}$		$Z_{Line\,23}$		$Z_{Line\,34}$		$Z_{Line\,45}$	
		$R_{Line\,1}$	0.35Ω	$R_{Line\,2}$	0.35Ω	$R_{Line\,3}$	0.35Ω	$R_{Line\,4}$	0.35Ω
		$L_{Line\,1}$	0.07mH	$L_{Line\,2}$	0.07mH	$L_{Line\,3}$	0.07mH	$L_{Line\,4}$	0.07mH
Loads		**Load 1**		**Load 2**		**Load 3**	**Load 4**	**Load 5**	
		$R = 300\Omega$		$R = 40\ \Omega$		$R = 50\ \Omega$	$R = 50\ \Omega$	$R = 50\ \Omega$	
		$L = 477\text{mH}$		$L = 64\ \text{mH}$		$L = 64\ \text{mH}$	$L = 64\ \text{mH}$	$L = 95\ \text{mH}$	

t= 2s. It restores the operating output terminal voltage and frequency in short time duration. Further, at t=3s, load of $R = 300\ \Omega$ and $L = 47\text{mH}$ is added to load 1, and at t=4s, load connected to DG 3 is switched off. The results in figure 5 and figure 6 show that the voltage and frequency restored to the nominal values very quickly after controller activation and maintained within permissible limits after experiencing slight deviations at small signal disturbances i.e., load variation. For simulation all the communication links are subjected to AWGN with $\sigma^2 = 10^{-2}$ and link delay of 100ms.

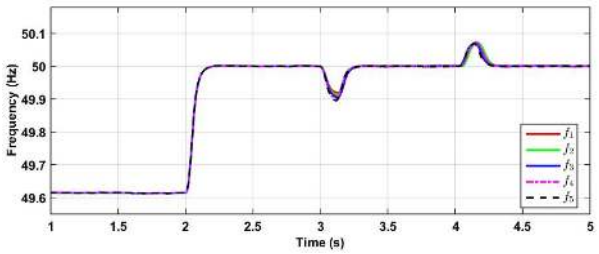

Figure 5. Frequency restoration Performance

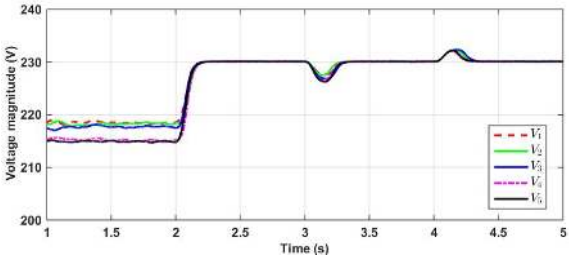

Figure 6. Voltage restoration Performance

5.2. Plug and Play (PNP) operation

The presented control methodology is evaluated for PNP case study in this subsection. The DG 5 is switched off and switched on again intentionally at t=3s and t=4s respectively. The communication topology for PNP operation is shown in figure 7. The obtained simulation results given in figure 8 and figure 9 depict the efficacy of presented control method for PNP operation and the voltage and frequency are maintain within permissible limit during high signal disturbance i.e., DG disconnection. The result in figure 10 and figure 11 show that, the total active and reactive power requirements are apportioned among DGs 1-4, while DG 5 is not associated to MG system. Also, operating output voltage and frequency are maintained within the nominal values i.e., 230 volts, 50 Hz with small transients at point of disturbance. Hence, presented scheme supports the PNP operation of LV MG network under noisy environment.

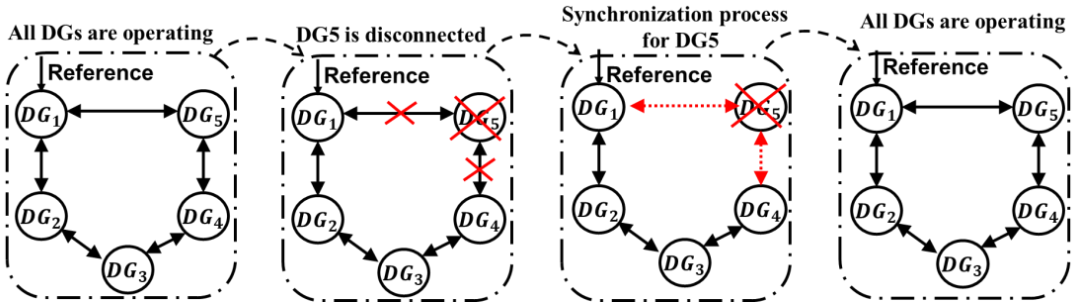

Figure 7. Communication graph for PNP operation

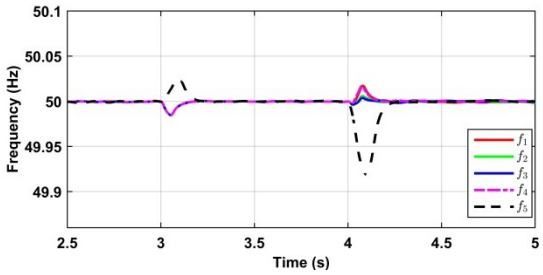

Figure 8. Frequency under PNP operation

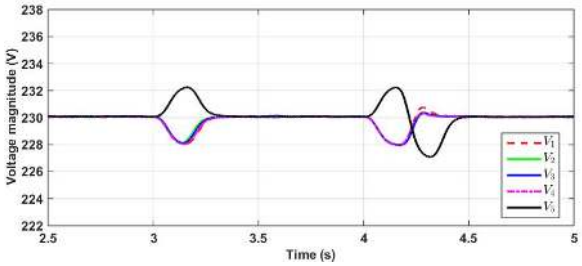

Figure 9. Voltage under PNP operation

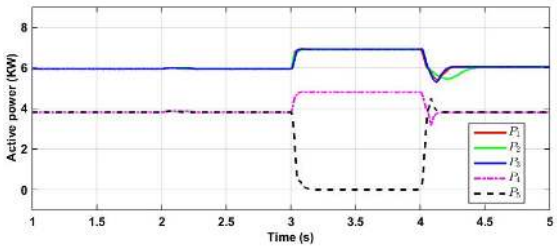

Figure 10. Active power under PNP operation

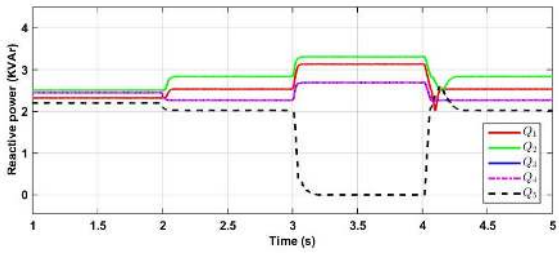

Figure 11. Reactive power under PNP operation

5.3. Robustness under variation in noise parameter

In this case study, the efficacy of the presented noise resilient secondary control method is evaluated under time- varying noise variance σ^2. The noise variance σ^2 varies in three stages: (a) $t \leq 2.5, \sigma^2 = 10^{-2}$; (b) $2.5 < t \leq 3.5, \sigma^2 = 10^{-1}$; and (c) $3.5 < t \leq 5, \sigma^2 = 0.3$. The results obtained in figure 12 and figure 13 clearly envisages the operating voltage magnitude and frequency of DGs are synchronized under permitted limit with different noise level respectively.

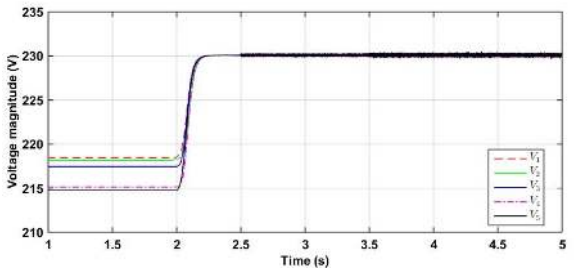

Figure 12. Voltage synchronizatio with time varying σ^2

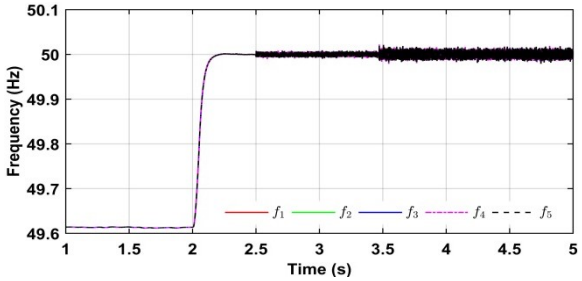

Figure 13. Frequency synchronization with time varying σ^2

6. Conclusion

The work presented in this paper deals with noisy communication links in secondary control layer. A noise resilient distributed secondary control methodology for a low voltage islanded MG network. This work considers a low voltage grid where the lines are dominantly resistive in nature and the information sharing communication channels among the DGs are corrupted with AWGN. The presented a primary droop-boost control augmented with noise resilient distributed secondary control scheme to restore the DG operating output terminal voltage and frequency while providing definitive real power sharing in finite time. Further, the control presented is self-reliant and does not depend on the noise type and required only neighbours information for control and corrective signal, hence can be implemented over a minimal communication network with connected graph. The stability proof is derived using rigorous Lyapunov analysis while considering complete nonlinear dynamics of LV MG network. The simulation results shows that the presented method envisage robust and resilience performance even during load perturbation, loss of DG unit and time varying noise parameter variation. The accurate reactive power sharing is still a problem for future consideration for authors along with extension of presented work for hybrid AC/DC MG and DC microgrid.

References

[1] Guo F, Wen C, Mao J, and Song Y-D 2015 Distributed secondary voltage and frequency restoration control of droop-controlled inverter-based microgrids *IEEE Transactions on Industrial Electronics* **62**(7) pp 4355–4364

[2] Guerrero J M, Vasquez J C, Matas J, Vicuna L G De, and Castilla M 2011 Hierarchical control of droop-controlled ac and dc microgridsa general approach toward standardization *IEEE Transactions on Industrial Electronics* **58**(1) pp 158–172

[3] Bidram A and Davoudi A 2012 Hierarchical structure of microgrids control system *IEEE Transactions on Smart Grid* **3**(4) pp 1963–1976

[4] Shafiee Q, Guerrero J M, and Vasquez J C 2014 Distributed secondary control for islanded microgridsa novel approach *IEEE Transactions on Power Electronics* **29**(2) pp 1018–1031

[5] Li Z, Zang C, Zeng P, Yu H, and Li H 2016 Mas based distributed automatic generation control for cyber-physical microgrid system *IEEE/CAA Journal of Automatica Sinica* **3**(1) pp 78–89

[6] Shrivastava S, Subudhi B and Das S 2018 Distributed voltage and frequency synchronisation control scheme for islanded inverter-based microgrid *IET Smart Grid* **1**(2) pp 48–56

[7] Bidram A, Lewis FL and Davoudi A 2014 Distributed control systems for small scale power networks: Using multiagent cooperative control theory *IEEE Control Systems* **34**(6) pp 56–77

[8] N L Soultanis, S A Papathanasiou and N D Hatziargyriou 2007 A Stability Algorithm for the Dynamic Analysis of Inverter Dominated Unbalanced LV Microgrids *IEEE Transactions on Power Systems* **22**(1) pp 294-304
[9] Bidram A, Davoudi A, Lewis FL and Guerrero JM 2013 Distributed cooperative secondary control of microgrids using feedback linearization *IEEE Transactions on Power Systems* **28**(3) pp 3462–3470
[10] Dehkordi NM, Baghaee HR, Sadati N and Guerrero J M 2019 Distributed noise-resilient secondary voltage and frequency control for islanded microgrids *IEEE Transactions Smart Grid* **10**(4) pp 3780–3790
[11] Romero ME and Seron MM 2019 Ultimate boundedness of voltage droop control with distributed secondary control loops *IEEE Transactions Smart Grid* **10**(4) 4107–4115
[12] Liu S, Wang X and Liu PX 2015 Impact of communication delays on secondary frequency control in an islanded microgrid *IEEE Transactions Industrial Electronics* **62**(4) pp 2021–2031
[13] Hu J and Feng G 2010 Distributed tracking control of leader–follower multi-agent systems under noisy measurement *Automatica* **46**(8) pp 1382–1387
[14] Shrivastava S, Subudhi B and Das S 2018 Noise-resilient voltage and frequency synchronisation of an autonomous microgrid *IET Generation, Transmission & Distribution* **13**(2) pp 189-200
[15] Shrivastava S, Subudhi B and Das S 2017 Voltage and frequency synchronization of a low voltage inverter based microgrid *4th International Conference on Power, Control & Embedded Systems (ICPCES)* IEEE pp 1-6